ACS OMEGA

http://pubs.acs.org/journal/acsodf

Article

3D Printing-Assisted Supramalleolar Osteotomy for Ankle Osteoarthritis

Changgui Zhang, Yangjing Lin, Liu Yang, and Xiaojun Duan*

Cite This: *ACS Omega* 2022, 7, 42191−42198

Read Online

ACCESS | Metrics & More | Article Recommendations | Supporting Information

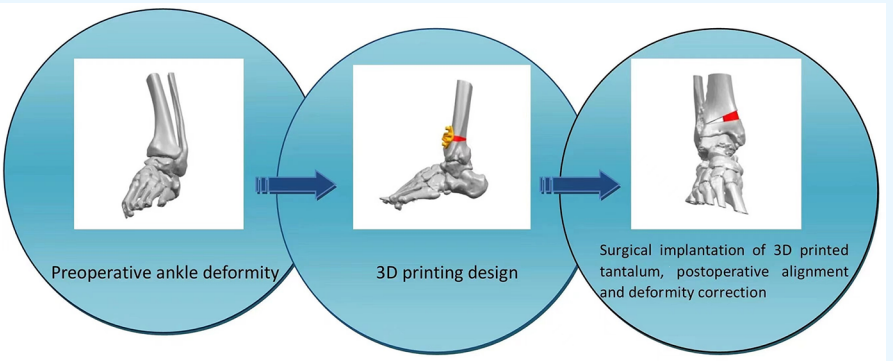

ABSTRACT: Ankle osteoarthritis (OA) is an important factor that causes pain and dysfunction after ankle joint movement. In early and mid-term ankle OA, supramalleolar osteotomy can delay the progression of disease and maximize the preservation of ankle joint function. Three-dimensional printing (3DP) technology has brought us new hope, which can improve the accuracy of osteotomy, reduce the number of fluoroscopy, reduce the amount of blood loss, and achieve personalized and accurate treatment. The data of 16 patients with ankle OA in our center from January 2003 to July 2020 were retrospectively analyzed and divided into the 3DP group and the traditional group according to different treatment methods. Seven patients in the 3DP group used the 3DP personalized osteotomy guide; nine patients were treated by traditional osteotomy. All patients were followed up for 13.9 ± 3.1 months after the operation. The operation time in the 3DP group was 126.4 ± 11.1 min, its intraoperative blood loss was 85.7 ± 24.1 mL, and its intraoperative fluoroscopy time was 2.4 ± 0.2, which were all significantly less than 167.3 ± 12.2 min, 158.3 ± 22.8 mL, and 5.8 ± 0.2 times in the traditional group ($P < 0.05$), respectively. In the 3DP group, its postoperative tibial anterior surface (TAS) angle was 90.6 ± 0.3° and the talar tilt (TT) angle was 2.2 ± 0.6°, which were all significantly different compared with its preoperative data of 83.4 ± 1.7 and 8.0 ± 1.5°, respectively ($P < 0.05$). Compared with traditional osteotomy, 3DP-assisted supramalleolar osteotomy for varus and valgus ankle OA can significantly shorten the operation time and reduce intraoperative bleeding and the frequency of intraoperative fluoroscopy; personalized 3DP osteotomy guides and models can assist in the accurate correction of varus deformity during operation, restore the lower limb alignment, and improve the biomechanical status of the lower limbs. In addition, the 3DP of porous tantalum has good histocompatibility, and its interface structure and porosity are more conducive to bone ingrowth. For complex bone defects and revision prostheses, matching implants can be printed individually, which could realize the personalized precise treatment.

INTRODUCTION

Ankle osteoarthritis (OA) is an important factor that causes pain and dysfunction in the ankle joint. Today, approximately 1% of adults in the world suffer from ankle OA.[1−3] When standing, the ankle joint bears a load equivalent to 5 times the weight of the whole body. The joint deformity caused by degeneration or distal tibial or fibular fracture will make the contact surface between the tibia and the talus reduced, and the load stress on the remaining contact surface increased, thus changing the load distribution and joint coordination and resulting in the wear and damage of articular cartilage, which can easily develop into chronic pain, ankle dysfunction, and eventually ankle OA. End-stage ankle OA requires ankle joint arthrodesis or ankle arthroplasty.[4] Although pain can be relieved, the mobility of the ankle is impaired. In early- and mid-stage ankle OA, the performance of supramalleolar osteotomy can delay the progression of ankle OA. It can adjust the spatial relationship between the talus and tibia,

Received: August 4, 2022
Accepted: October 26, 2022
Published: November 8, 2022

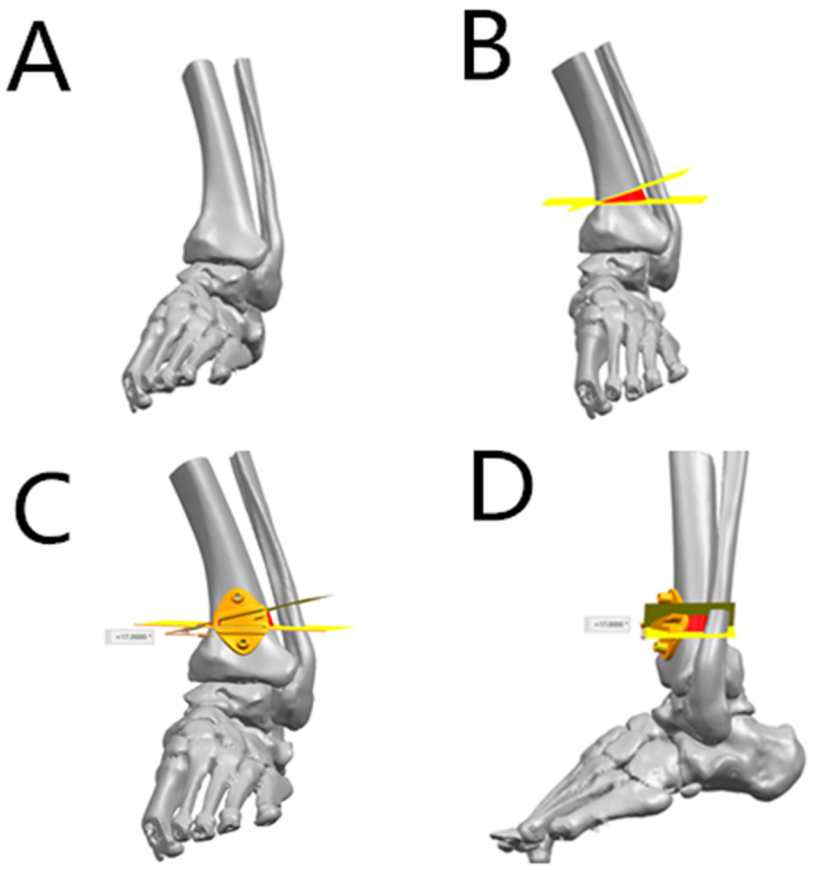

Figure 1. 3D model of the ankle joint. (A) Reconstruct the 3D model of the ankle joint based on the CT data. (B) Calculate the amount of osteotomy, the size of the bone defect, and the preparation of the surgical guide; design the tantalum metal implant. (C) Design the surgical guide for the osteotomy (anteroposterior view). (D) Design the surgical guide for the osteotomy (lateral view).

redistribute the load in the ankle joint, correct the lower limb alignment, maximize the preservation of ankle joint function, and delay the progression of ankle OA.[5] In recent years, with the rapid development of three-dimensional printing (3DP) technology, this new technology has been widely used in medical fields such as orthopedics and oral and maxillofacial surgery.[6,7] Applying 3D printing technology to ankle osteotomy and making osteotomy guides can improve the accuracy of osteotomy, reduce the number of fluoroscopy, reduce the amount of blood loss, and shorten the learning curve of surgeons. Besides, according to the specific osteotomy method, 3D-printed tantalum metal can be applied to large bone defects, avoiding complications of autologous bone transplantation. Recent studies have shown that personalized surgical guides can improve the accuracy of osteotomy, reduce the number of fluoroscopy times, reduce intraoperative bleeding, and shorten the surgeon's learning curve.[8] Besides, for large bone defects, the application of 3DP tantalum metal can avoid the trauma of autologous graft.

We conducted a retrospective study on the data of 16 patients with ankle OA treated in our center from Jan 2003 to July 2020 and compared the efficacy of 3DP-assisted supramalleolar osteotomy with traditional methods to analyze the advantages of the 3DP personalized guide in the osteotomy and promote the application of this technique.

MATERIALS AND METHODS

Inclusion Criteria and Exclusion Criteria. Case inclusion criteria: (i) patients with traumatic and degenerative ankle OA; (ii) mild to moderate varus and valgus; (iii) mild or moderate ankle OA; and (iv) clinical symptoms such as pain in walking and limitation of daily activities. Case exclusion criteria: (i) patients with severe ankle joint infection; (ii) patients with severe coagulation dysfunction or severe cardiovascular and cerebrovascular diseases; (iii) severe osteoporosis; and (iv) patients with neuromuscular diseases or severe malformations.

A total of 16 patients were enrolled in this study, and they were divided into two groups according to different treatment methods: 7 patients were treated with a 3DP personalized osteotomy guide (3DP group), including 3 males and 4 females, 2 cases of left ankle and 5 cases of right ankle, and aged 47.1 ± 7.9 years; 9 patients were treated with traditional osteotomy (traditional group), including 4 males and 5 females, 6 cases of left ankle and 3 cases of right ankle, and aged 34.7 ± 4.3 years. All operations were performed by the same two senior surgeons. This study was approved by the Ethics Committee of Southwest Hospital, Third Military Medical University (Army Medical University) (no. (B)-KY20211159), and all patients signed an informed consent form and agreed to be included in the study.

Preoperative Personalized Application of the 3DP Technology. In the 3DP group, a 1:1 model of the lesion and personalized surgical guide was prepared. The 3D computed tomography (CT) thin-layer scan (Siemens, Germany) of the ankle osteotomy was routinely conducted, and the CT scan thickness was 1 mm. The digital imaging and communications in medicine (DICM) data were extracted and imported into the model intestinal microflora in computer simulation

https://doi.org/10.1021/acsomega.2c04764
ACS Omega 2022, 7, 42191−42198

(MIMICS) software to reconstruct the 3D data of the lesion and its surrounding tissues. The MIMICS-reconstructed data were then imported into the 3D design software SIEMENS NX (Siemens PLM Software, Germany). Under the guidance of the surgeon, the engineers designed the personalized guide system for supramalleolar osteotomy according to the alignment and degree of deformity of the lower limbs and calculated the amount of iliac bone to be grafted. The personalized 3DP guides were designed according to the anatomical landmarks to perfectly match the bone surface, and the center of the guide contained guide holes for the Kirschner wire to drill (Figure 1A,B). The data of the designed guides were converted into STL format and imported into a 3D printer (model: UP BOX, Tiertime, China; Video S1) for printing. Poly(lactic acid) (Tiertime, China) was used as a raw material to prepare the individualized guides (Figures 1 and 2),

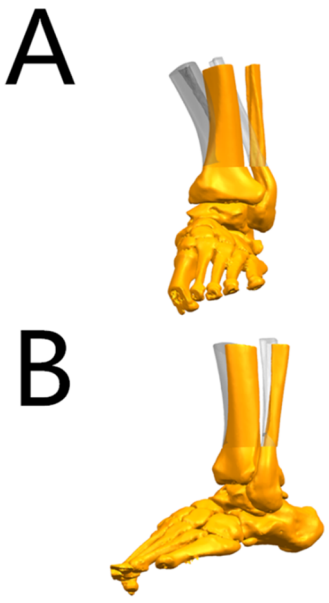

Figure 2. 3D model of the ankle joint. (A) Simulate the correction after osteotomy, compare it with the original tibia position, and observe the alignment and the biomechanics of the lower limb (anteroposterior view). (B) Simulate the correction after osteotomy, compare it with the original tibia position, and observe the alignment and the biomechanics of the lower limb (lateral view).

and lesion models were prepared. The personalized porous tantalum implants were designed and printed out according to the size of the bone defect. The porosity of the 3DP porous tantalum is 75%. When preparing the lesion model, different colors can be used to distinguish the lesion from the surrounding healthy tissue, which is conducive to surgical rehearsals and perfection of the surgical plans. The guide, model, and tantalum metal were sealed and sterilized with ethylene oxide for intraoperative use.

Surgical Techniques. After successful anesthesia, the patient took a supine position with a tourniquet on the root of the thigh. Draping and sterilization were routinely conducted, and then the tourniquet pressure was set to 300 mmHg. An incision of about 8 cm was cut on the medial malleolus of the affected limb to fully expose the distal tibia; the nerves and blood vessels remained protected during the process. Before osteotomy, Kirschner wire and C-arm fluoroscopy were applied for intraoperative positioning; the wires were drilled from the medial anterior to the lateral posterior. After further confirmation by the C-arm fluoroscopy, a pendulum saw was used for osteotomy. In the 3D printing group, the osteotomy surface of the distal tibia was determined with the aid of the 3DP guide and model. Two Kirschner wires were drilled for fixation. C-arm fluoroscopy was applied for confirmation of the osteotomy position and depth. A pendulum saw was used to cut off the medial, anterior, and posterior cortical bones of the tibia while retaining the lateral cortical bone. For patients with severe deformities, fibula osteotomy was required first. An 8 cm incision was made at the lateral distal end of the affected shank to fully expose the distal fibula. In the traditional group, C-arm fluoroscopy was used for fibular osteotomy. In the 3D printing group, the 3DP guide was used to assist the distal fibula osteotomy. The osteotomy position was maintained at a position of 90° of dorsiflexion and 5° of valgus. In the traditional group, an appropriate size of autologous ilium was obtained according to the intraoperative conditions. In the 3D printing group, an osteotome and an expander were used to determine the size of the bone graft required based on the preoperative 3DP model and the calculated amount of iliac bone. The iliac bone on the same side was taken out and trimmed with a small pendulum saw, and the incision was sutured. The trimmed iliac bone was grafted to the osteotomy surface of the medial tibia; allograft bone granules were used to fill the gap. If the patient had a large bone defect, 3DP personalized porous tantalum metal could be implanted. Steel plates were placed on the distal end of the tibia and fibula, and the length of the screws was premeasured. After reaming along the guide pin, the screws were screwed in. The C-arm fluoroscopy showed that the bone pieces were aligned, and the position of the internal fixation screws was satisfactory. The incision was washed with a large amount of saline, the instruments and gauze were counted to make sure they were correct, and then a drainage tube was placed. The incision was sutured layer by layer, and the ankle joint was fixed with plaster after compressing with sterile dressing and elastic bandage.

Postoperative Treatment. After anesthesia disappears, the patient could start toe activities and was guided to perform functional exercises. The drainage tube was pulled out 24 h after surgery, antibiotics were injected for 48 h, and full rest was adopted for 2 weeks. The lower limbs were fixed in plaster for 6 weeks, and weight bearing was forbidden. Functional exercise was performed strictly in accordance with the instructions. At 6 weeks, patients were re-examined, and the perioperative complications were recorded. Regular re-examinations at the outpatient were conducted.

Indicators. The operation time, the number of C-arm X-ray fluoroscopy times, and the amount of intraoperative blood loss were recorded. Radiographs of the ankle joint were taken before surgery and at the follow-ups, and the preoperative and postoperative imaging data of the tibial anterior surface angle (TAS), the talar tilt angle (TT), and the tibial lateral surface angle (TLS) were measured and recorded. All imaging measurements were performed independently by two attending physicians. If there were differences in the measurement results, an associate chief physician would evaluate the value.

Statistical Analysis. The measuring data adopted the mean ± standard deviation and were analyzed by SPSS 22.0 (SPSS Inc., IBM). For the comparison of the various indicators between the 3DP group and the traditional group, as well as between the preoperative and postoperative data in the 3DP

https://doi.org/10.1021/acsomega.2c04764
ACS Omega 2022, 7, 42191−42198

Table 1. Comparison of the Operation Time, Intraoperative Blood Loss, Number of Fluoroscopy Times, Postoperative TAS, TT, and TLS between the Two Groups ($\bar{x} \pm s$)

group	cases (n)	operation time (min)	intraoperative blood loss (mL)	intraoperative number of fluoroscopy (times)	TAS (degree)	TT (degree)	TLS (degree)
3DP group	7	126.4 ± 11. 1	85.7 ± 24.2	2.4 ± 0.2	90.6 ± 0.3	2.2 ± 0.6	83.9 ± 0.2
traditional group	9	167.3 ± 12.2	158.3 ± 22.8	5.8 ± 0.2	89.8 ± 0.4	1.8 ± 0.4	83.7 ± 0.2
t value		2.40	2.16	14.0	1.92	0.64	0.59
P value		<0.05	<0.05	<0.05	>0.05	>0.05	>0.05

group, if the data conformed to normal distribution, the t test would be used; if the data conformed to non-normal distribution, the rank sum test would be used. $P < 0.05$ was considered statistically significant.

RESULTS

All surgeries for the 16 patients were successfully completed. Patients were followed up for an average of 13.9 ± 3.1 months after surgery. The operation time in the traditional group was 167.3 ± 12.2 min, the intraoperative blood loss was 158.3 ± 22.8 mL, and the number of intraoperative fluoroscopy was 5.8 ± 0.2 times, which were all significantly more than 126.4 ± 11.1 min, 85.7 ± 24.2 mL, and 2.4 ± 0.2 times in the 3DP group ($P < 0.05$), respectively (Table 1). Compared with the traditional group, there was no statistically significant difference in TAS, TT, and TLS in the 3DP group postoperatively ($P > 0.05$). In the 3DP group, the preoperative TAS was 83.4 ± 1.7° and TT was 8.0 ± 1.5°, which all had statistically significant differences with the postoperative data of (90.6 ± 0.3, 2.2 ± 0.6°, $P < 0.05$); the preoperative TLS was 84.5 ± 0.1°, which had no statistically significant differences with the postoperative data of 83.9 ± 0.2° ($P > 0.05$) (Table 2). During the follow-up period, none of the 16 patients had complications such as internal fixation loosening, displacement, and wound infection. 3DP of porous tantalum has good histocompatibility, with its interface structure and porosity more conducive to bone ingrowth. For complex bone defects and revision prostheses, matching implants can be printed individually, thus realizing personalized precise treatment (see Figures 3−5 for typical cases).

Table 2. Comparison of Preoperative and Postoperative TAS, TT, and TLS in Patients with Varus and Valgus Ankle OA in the 3DP Group ($n = 7$)[a]

time points	TAS (degree)	TT (degree)	TLS (degree)
preoperative	83.4 ± 1.7	8.0 ± 1.5	84.5 ± 0.1
postoperative	90.6 ± 0.3	2.2 ± 0.6	83.9 ± 0.2
t value	4.10	4.30	2.30
P value	<0.05	<0.05	>0.05

[a]TAS, tibial anterior surface angle; TT, talar tilt angle; TLS, tibial lateral surface angle.

DISCUSSION

About 15% of the world's adults are affected by joint pain caused by OA, and about 1% of people suffer from ankle OA. Compared with patients with hip and knee arthritis, young people have a higher incidence of ankle OA. Post-traumatic malunion, bone graft disorders, congenital or metabolic diseases, and degenerative arthritis can cause deformity of the distal tibia. The deformity would cause an uneven load on the talar surface, causing damage to the articular cartilage and leading to ankle OA. Since the weight-bearing area of the ankle joint is smaller than that of the knee joint and the load per unit area is greater, ankle OA is more likely to develop. End-stage ankle OA can only be treated by ankle arthrodesis and ankle arthroplasty, which will cause loss of ankle joint mobility. Therefore, for ankle OA, surgery should be performed as soon as possible. Supermalleolar osteotomy can treat varus and valgus ankle OA; its purpose is to restore the alignment, correct the deformity, and redistribute the load in the ankle joint, thereby improving the biomechanics of the lower limbs and delaying the progression of ankle OA.[9]

As a joint-preserving osteotomy, supermalleolar osteotomy has been proved by many studies to be able to improve the ankle joint function and relieve pain. In 1995, Takakura et al.[10] systematically reported the prognosis of patients with supermalleolar osteotomy for the first time. They found that supermalleolar osteotomy was an effective way to treat mid-term ankle OA and could delay the progression of ankle OA. Giannini et al.[11] reported 22 cases of valgus deformity due to ankle joint fractures who underwent supermalleolar osteotomy. After 5 years of follow-up, the average American Orthopaedic Foot and Ankle Society (AOFAS) score increased from 45 points preoperatively to 87 points postoperatively, and 20 cases of post-traumatic ankle deformity were corrected. Colin et al.[12] performed supermalleolar osteotomy on 83 patients with early-stage ankle OA induced by post-traumatic ankle deformity. They followed up the patients for an average of 3.5 years and found that supermalleolar osteotomy had satisfactory results for ankle OA combined with varus or valgus deformities. The patients' AOFAS scores increased, the ankle joint function improved, the progression of the post-traumatic arthritis was delayed, and ankle arthrodesis or ankle arthroplasty was avoided. Krähenbühl et al.[13] performed supermalleolar osteotomy on 44 patients with varus post-traumatic ankle OA. They studied the prognosis of early- and mid-stage ankle OA and found that the treatment efficacy of supermalleolar osteotomy was better for patients in stages 2B and 3A of ankle OA than those in stage 3B. They also confirmed that supermalleolar osteotomy was an effective method for treating early- and mid-stage traumatic varus ankle OA.

In traditional osteotomy, surgeons usually perform the osteotomy based on their previous clinical experience. During the operation, it is necessary to adjust the position and angle of the osteotomy with repeated fluoroscopy, which would lead to more bone loss, prolonged operation time, more intraoperative blood loss, and increased postoperative complications, reducing the effect of surgery. 3D printing is a revolutionary technology and is developing at a rapid rate.[14−22] It can be used for the 3D reconstruction model, which is more specific, vivid, and accurate. Surgeons can analyze the lesions via the 3D model, design surgical plans, and measure the osteotomy angle and direction. The lesion model can also be printed out for the

https://doi.org/10.1021/acsomega.2c04764
ACS Omega 2022, 7, 42191−42198

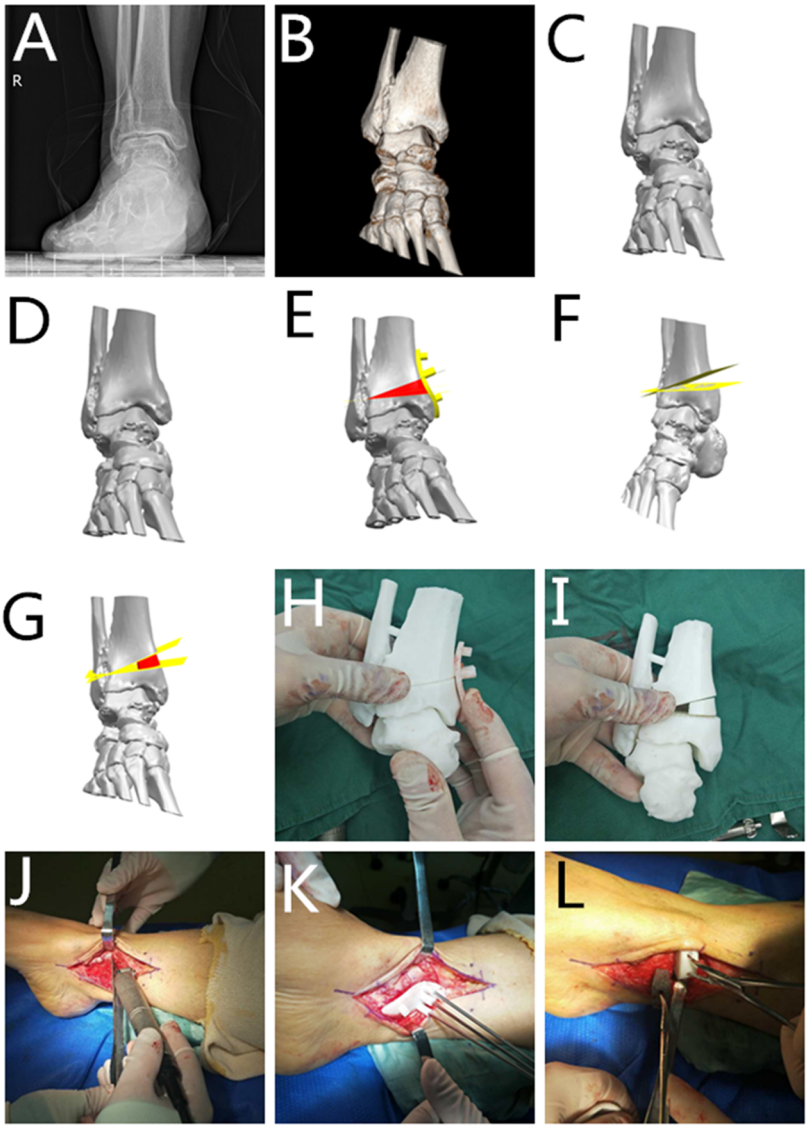

Figure 3. Typical case. (A) Preoperative radiograph (anteroposterior view). (B) Preoperative radiograph (lateral view). (C) Preoperative 3D reconstruction. (D) 3D reconstruction of the ankle joint based on CT data. (E) Calculate the osteotomy amount and bone defect size; design the 3DP guide and simulate the osteotomy process. (F) Simulate the osteotomy process and calculate the osteotomy amount. (G) Design the tantalum metal according to the osteotomy amount and bone defect size; simulate the postimplantation situation; (H, I) apply the 3DP model and guide during the operation to formulate the surgical plan. (J) Locate the position of the osteotomy according to the 3DP model. (K) Perform the osteotomy according to the 3DP model and guide during the operation. (L) Compare the actual osteotomy amount with the preoperative calculation.

surgeons to perform surgical rehearsals to make the actual operation smoother, thus shortening the surgeons' learning curve. The 3DP surgical guide is a personalized aid specially customized according to the surgical needs of the patient before surgery, which is a good link between the preoperative design and the surgical operation. The guide can be tailored according to the patient's own situation, and it can guide the position, angle, and direction of the intraoperative osteotomy to ensure the accuracy of the surgery. In the field of joint surgery, the application of personalized guide is under continuous exploration and development. Most studies have shown that the use of surgical guides to assist orthopedic surgery can achieve satisfactory clinical results.[18] Duan et al.[4] applied 3DP personalized surgical guides to assist ankle arthrodesis and found that it could shorten the operation time and reduce intraoperative radiation and bleeding. Zheng et al.[22] used 3DP templates to navigate the proximal femoral osteotomy for 12 children with developmental dysplasia of the hip and found that the 3DP guides could shorten the operation time, reduce intraoperative blood loss, improve the accuracy of osteotomy and accuracy of prosthesis position, and significantly improve the lower limb alignment. In addition, the surgical guide could also reduce the number of intraoperative fluoroscopy times, which was beneficial to protect patients and medical care personnel. Yang et al.[20] conducted 3DP-assisted osteotomy for the malunion of lateral tibial plateau fracture on seven patients and found that the 3DP technology could help accurately design the surgery, reduce intraoperative blood loss, shorten surgery time, and reduce the risk of postoperative deformity. Shi et al.[19] utilized 3D navigation for closing-wedge distal femoral osteotomy on 12 cases of patients with valgus knee joint deformity. They found that using 3DP technology

https://doi.org/10.1021/acsomega.2c04764
ACS Omega 2022, 7, 42191−42198

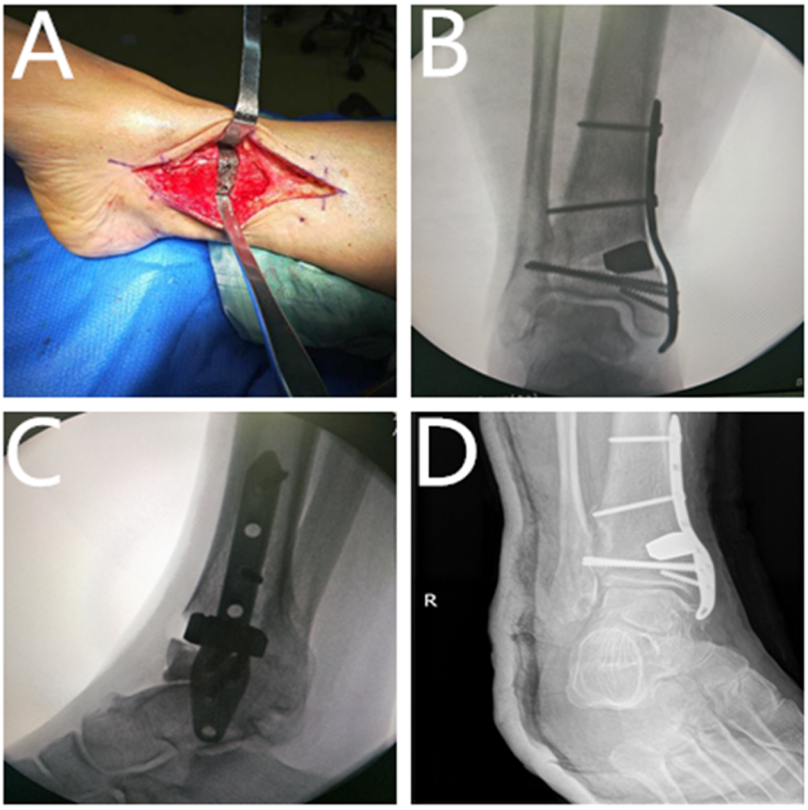

Figure 4. Typical case. (A) Implant the tantalum metal. (B) The intraoperative radiograph shows good correction position (anteroposterior view). (C) The intraoperative radiograph shows good correction position (lateral view). (D) The re-examined radiograph at 15 days postoperatively (anteroposterior view).

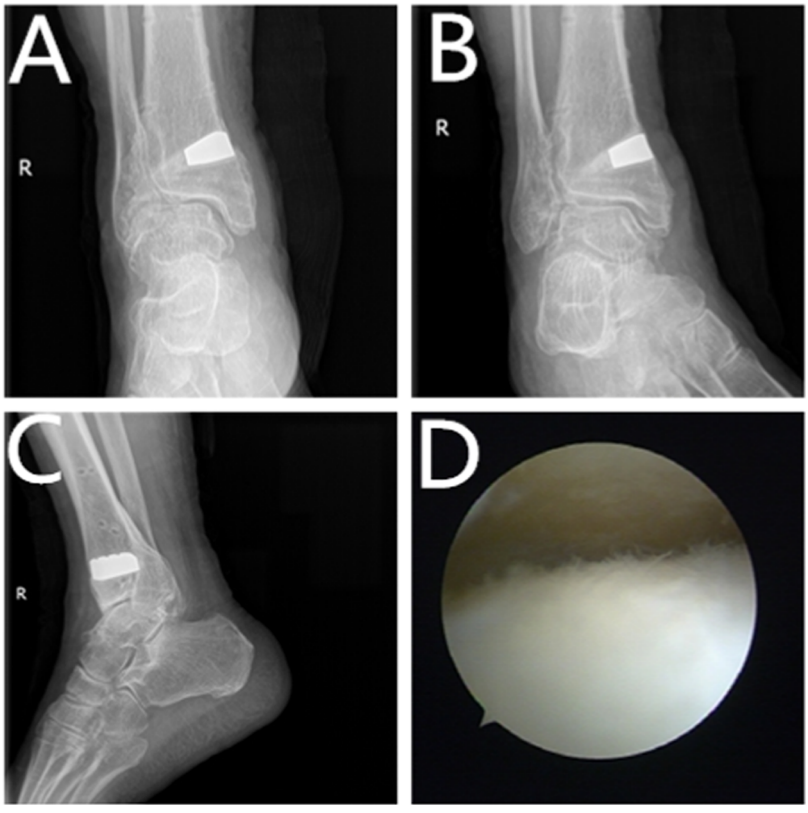

Figure 5. Typical case. (A) Radiograph of the ankle joint at 1.5 years, anteroposterior view. (B) Radiograph of the ankle joint at 1.5 years, mortise view. (C) Lateral radiograph at 1.5 years. (D) Re-examination of arthroscopy at 1.5 years showed reduced cartilage degeneration.

https://doi.org/10.1021/acsomega.2c04764
ACS Omega 2022, 7, 42191−42198

for osteotomy could improve accuracy, enhance efficiency, and reduce intraoperative fluoroscopy times, thus achieving personalized and precise treatment. The 3DP technology has realized the transformation from traditional empirical medicine to precision medicine.

Besides, we can also use 3D reconstruction technology to calculate the specific amount of osteotomy before surgery. If bone grafting is needed, the amount of bone defect can be calculated preoperatively, and different surgical methods can be used according to the size of the bone defect. For small bone defects, autologous iliac bone grafting or allogeneic bone grafting can be performed. In traditional surgery, to obtain a suitable iliac bone, it would require repeated confirmation of the C-arm fluoroscopy during the operation, causing large trauma and bleeding. The 3DP technology, which can calculate the defect size before surgery, can obtain the accurate amount of iliac bone. For large bone defects, we can perform 3DP tantalum metal implantation according to the specific bone amount, avoiding the complications of taking large pieces of autologous bone and grafting. Titanium alloys have been widely used in orthopedics, but due to a lack of good corrosion resistance and osseointegration ability, they often require surface coating to enhance their biological activity and corrosion resistance. And tantalum metal has better corrosion resistance and osseointegration ability.[23,24] Our previous research also confirmed that porous tantalum could provide mechanical strength, reduce stress shielding, and facilitate stress conduction.[25] Tantalum metal has particularly good biocompatibility, and porous tantalum structure is very conducive to osteogenesis. Its elasticity is close to that of human bones. During the 1.5-year follow-up, the patient had no local erythema and swelling, and the incision healed well. Laboratory examinations showed that the patients' erythrocyte sedimentation rate and C-reactive protein were within the normal range, and the tantalum metal had good biocompatibility and did not cause immune rejection.

The best porosity of porous tantalum is 75−85%, which can improve tissue permeability and promote nutrient exchange in the scaffold. In addition, the pore size has an important impact on the ingrowth tissue properties. If the pore is too large, the stability of tantalum metal and bone would not be good. However, fibrous tissue can only be formed in a pore diameter of <50 μm. The porous tantalum structure with a pore diameter ranging from 400 to 600 μm is conducive to the ingrowth of bone tissue, and bone tissue can be observed inside the porous structure.

Porous tantalum has a porosity of 75−85%. The high porosity structure gives excellent mechanical properties to porous tantalum. Its maximum bending strength is 110 MPa, which can provide support for new bone tissue. In addition, the elastic modulus of porous tantalum is between the cortical bone and cancellous bone. This elastic modulus that can match with human bone tissue can effectively reduce the stress shielding effect. The friction coefficient of porous tantalum is 0.80 and 0.74 for cancellous bone and cortical bone, respectively. The friction coefficient between porous tantalum and bone tissue is 40−80% higher than that of traditional metal materials, which helps to combine the implant with the host bone interface and enhance the stability at the initial stage of implantation.

3DP can realize a bionic trabecular bone structure. By adjusting the porous structure parameters, it can make its elastic modulus between the cancellous bone and cortical bone to avoid stress shielding and improve the initial stability of porous tantalum implant; the bionic trabecular bone structure induces the growth of new bone tissue while improving the long-term stability of the implant. We found for the first time that the interface structure and porosity of 3DP porous tantalum are more conducive to bone ingrowth, creating a better environment. Next, the 3DP of joint prostheses can be realized. Compared with traditional prostheses, it not only matches more to the bone in terms of appearance and shape but is also more conducive to the control of porosity and 3D structure. For complex bone defects and revision prostheses, matching implants can be printed individually, realizing personalized and precise treatment.[26−28]

In recent studies, tantalum metal implants all showed very good results, which could avoid complications such as pain, nerve damage, infection, and large sequestrum caused by iliac bone removal and implantation of large allograft bone. In the reconstruction of the foot and ankle joints, Papadelis et al.[14] reported 18 cases who underwent subtalar block arthrodesis using porous tantalum metal implants, and all 18 patients (100%) completed the arthrodesis within the average follow-up period of 17.7 months.

Limitations. However, this study still has some deficiencies, such as a comparatively small number of cases and relatively short follow-up period. Future mid- and long-term follow-up studies need to be conducted to overcome these deficiencies.

CONCLUSIONS

In summary, the results of this study show that the 3DP-assisted supermalleolar osteotomy can accurately correct varus and valgus deformities, restore the lower limb alignment, and improve the biomechanics of the lower limb. Compared with traditional osteotomy, the 3DP-assisted osteotomy can shorten the operation time and reduce the amount of intraoperative blood loss and the number of intraoperative fluoroscopy times. It can achieve accurate osteotomy, improve the efficiency and safety of the operation with preoperative surgical planning, and realize the personalized and precise treatment. In addition, the 3DP of porous tantalum has good histocompatibility; for complex bone defects and revision prostheses, matching implants can be printed individually, which could realize the personalized precise treatment.

ASSOCIATED CONTENT

Supporting Information

The Supporting Information is available free of charge at https://pubs.acs.org/doi/10.1021/acsomega.2c04764.

Data of the designed guides were converted into STL format and imported into a 3D printer for printing (MP4)

AUTHOR INFORMATION

Corresponding Author

Xiaojun Duan − *Center for Joint Surgery, Southwest Hospital, Third Military Medical University (Army Medical University), Chongqing 400038, China;* orcid.org/0000-0001-7644-2452; Email: duanxiaojun@hotmail.com

https://doi.org/10.1021/acsomega.2c04764
ACS Omega 2022, 7, 42191−42198

Authors

Changgui Zhang − *Center for Joint Surgery, Southwest Hospital, Third Military Medical University (Army Medical University), Chongqing 400038, China*

Yangjing Lin − *Center for Joint Surgery, Southwest Hospital, Third Military Medical University (Army Medical University), Chongqing 400038, China*

Liu Yang − *Center for Joint Surgery, Southwest Hospital, Third Military Medical University (Army Medical University), Chongqing 400038, China*

Complete contact information is available at: https://pubs.acs.org/10.1021/acsomega.2c04764

Funding

This work was financially supported by the China Ministry of Science and Technology National Key Research and Development Project (Grant No. 2016YFB1101404), the Chongqing Science and Health Joint Medical Research Surface Project (Grant No. 2021MSXM183), the Chongqing Postgraduate Education and Teaching Reform Research Project (Grant No. yjg203136), and the Talent Project of Chongqing Human Resources and Social Security Bureau (Grant No. CQYC20210101319).

Notes

The authors declare no competing financial interest.

■ ACKNOWLEDGMENTS

The authors thank Xin Chen from the Center for Joint Surgery, Southwest Hospital, Army Medical University, for the language support for this article.

■ REFERENCES

(1) Saltzman, C. L.; Salamon, M. L.; Blanchard, G. M.; Huff, T.; Hayes, A.; Buckwalter, J. A.; Amendola, A. Epidemiology of ankle arthritis: report of a consecutive series of 639 patients from a tertiary orthopaedic center. *Iowa Orthop. J.* **2005**, *25*, 44−46.

(2) Valderrabano, V.; Horisberger, M.; Russell, I.; Dougall, H.; Hintermann, B. Etiology of ankle osteoarthritis. *Clin. Orthop. Relat. Res.* **2009**, *467*, 1800−1806.

(3) Zhang, C.; Ao, Y.; Cao, J.; Yang, L.; Duan, X. Donor Cell Fate in Particulated Juvenile Allograft Cartilage for the Repair of Articular Cartilage Defects. *Am. J. Sports Med.* **2020**, *48*, 3224−3232.

(4) Duan, X. J.; Fan, H. Q.; Wang, F. Y.; He, P.; Yang, L. Application of 3D-printed Customized Guides in Subtalar Joint Arthrodesis. *Orthop. Surg.* **2019**, *11*, 405−413.

(5) Zhang, Y. Z.; Lu, S.; Zhang, H. Q.; Jin, Z. M.; Zhao, J. M.; Huang, J.; Zhang, Z. F. Alignment of the lower extremity mechanical axis by computer-aided design and application in total knee arthroplasty. *Int. J. Comput. Assisted Radiol. Surg.* **2016**, *11*, 1881−1890.

(6) Kim, H. J.; Park, J.; Shin, J. Y.; Park, I. H.; Park, K. H.; Kyung, H. S. More accurate correction can be obtained using a three-dimensional printed model in open-wedge high tibial osteotomy. *Knee Surg., Sports Traumatol., Arthroscopy* **2018**, *26*, 3452−3458.

(7) Kwun, J. D.; Kim, H. J.; Park, J.; Park, I. H.; Kyung, H. S. Open wedge high tibial osteotomy using three-dimensional printed models: Experimental analysis using porcine bone. *Knee* **2017**, *24*, 16−22.

(8) Duan, X.; He, P.; Fan, H.; Zhang, C.; Wang, F.; Yang, L. Application of 3D-Printed Personalized Guide in Arthroscopic Ankle Arthrodesis. *BioMed Res. Int.* **2018**, *2018*, No. 3531293.

(9) Chopra, V.; Stone, P.; Ng, A. Supramalleolar Osteotomies. *Clin. Podiatr. Med. Surg.* **2017**, *34*, 445−460.

(10) Takakura, Y.; Tanaka, Y.; Kumai, T.; Tamai, S. Low tibial osteotomy for osteoarthritis of the ankle. Results of a new operation in 18 patients. *J. Bone Jt. Surg., Br. Vol.* **1995**, *77*, 50−54.

(11) Giannini, S.; Faldini, C.; Acri, F.; Leonetti, D.; Luciani, D.; Nanni, M. Surgical treatment of post-traumatic malalignment of the ankle. *Injury* **2010**, *41*, 1208−1211.

(12) Colin, F.; Gaudot, F.; Odri, G.; Judet, T. Supramalleolar osteotomy: Techniques, indications and outcomes in a series of 83 cases. *Orthop. Traumatol.: Surg. Res.* **2014**, *100*, 413−418.

(13) Krähenbühl, N.; Akkaya, M.; Deforth, M.; Zwicky, L.; Barg, A.; Hintermann, B. Extraarticular Supramalleolar Osteotomy in Asymmetric Varus Ankle Osteoarthritis. *Foot Ankle Int.* **2019**, *40*, 936−947.

(14) Papadelis, E. A.; Karampinas, P. K.; Kavroudakis, E.; Vlamis, J.; Polizois, V. D.; Pneumaticos, S. G. Pneumaticos, S. G. Isolated Subtalar Distraction Arthrodesis Using Porous Tantalum: A Pilot Study. *Foot Ankle Int.* **2015**, *36*, 1084−1088.

(15) Jastifer, J. R.; Gustafson, P. A. Three-Dimensional Printing and Surgical Simulation for Preoperative Planning of Deformity Correction in Foot and Ankle Surgery. *J. Foot Ankle Surg.* **2017**, *56*, 191−195.

(16) Ren, X.; Yang, L.; Duan, X. J. Three-dimensional printing in the surgical treatment of osteoid osteoma of the calcaneus: A case report. *J. Int. Med. Res.* **2017**, *45*, 372−380.

(17) Schepers, T.; Misselyn, D. 3D Printing Calcaneal Fractures: Continuously Improving our Care by Making a Complex Problem Tangible. *J. Invest. Surg.* **2018**, *31*, 568−569.

(18) Sha, Y.; Wang, H.; Ding, J.; Tang, H.; Li, C.; Luo, H.; Liu, J.; Xu, Y. A novel patient-specific navigational template for anatomical reconstruction of the lateral ankle ligaments. *Int. Orthop.* **2016**, *40*, 59−64.

(19) Shi, J.; Lv, W.; Wang, Y.; Ma, B.; Cui, W.; Liu, Z.; Han, K. Three dimensional patient-specific printed cutting guides for closing-wedge distal femoral osteotomy. *Int. Orthop.* **2019**, *43*, 619−624.

(20) Yang, P.; Du, D.; Zhou, Z.; Lu, N.; Fu, Q.; Ma, J.; Zhao, L.; Chen, A. 3D printing-assisted osteotomy treatment for the malunion of lateral tibial plateau fracture. *Injury* **2016**, *47*, 2816−2821.

(21) Zhang, C.; Cao, J.; Zhu, H.; Fan, H.; Yang, L.; Duan, X. Endoscopic Treatment of Symptomatic Foot and Ankle Bone Cyst with 3D Printing Application. *BioMed Res. Int.* **2020**, *2020*, No. 8323658.

(22) Zheng, P.; Xu, P.; Yao, Q.; Tang, K.; Lou, Y. 3D-printed navigation template in proximal femoral osteotomy for older children with developmental dysplasia of the hip. *Sci. Rep.* **2017**, *7*, No. 44993.

(23) Welldon, K. J.; Atkins, G. J.; Howie, D. W.; Findlay, D. M. Primary human osteoblasts grow into porous tantalum and maintain an osteoblastic phenotype. *J. Biomed. Mater. Res., Part A* **2008**, *84*, 691−701.

(24) Tang, Z.; Xie, Y.; Yang, F.; Huang, Y.; Wang, C.; Dai, K.; Zheng, X.; Zhang, X. Porous tantalum coatings prepared by vacuum plasma spraying enhance bmscs osteogenic differentiation and bone regeneration in vitro and in vivo. *PLoS One* **2013**, *8*, No. e66263.

(25) Fan, H.; Deng, S.; Tang, W.; Muheremu, A.; Wu, X.; He, P.; Tan, C.; Wang, G.; Tang, J.; Guo, K.; et al. Highly Porous 3D Printed Tantalum Scaffolds Have Better Biomechanical and Microstructural Properties than Titanium Scaffolds. *BioMed Res. Int.* **2021**, *2021*, No. 2899043.

(26) Bobyn, J. D.; Stackpool, G. J.; Hacking, S. A.; Tanzer, M.; Krygier, J. J. Characteristics of bone in growth and interface mechanics of a new porous tantalum biomaterial. *J. Bone Jt. Surg., Br. Vol.* **1999**, *81*, 907−914.

(27) Kim, D.-G.; Huja, S. S.; Tee, B. C.; Larsen, P. E.; Kennedy, K. S.; Chien, H.; Lee, J. W.; Wen, H. B. Bone Ingrowth and Initial Stability of Titanium and Porous Tantalum Dental Implants. *Implant Dent.* **2013**, *22*, 399−405.

(28) Onggo, J. R.; Nambiar, M.; Onggo, J. D.; Tay, G.; Singh, P. J.; Babazadeh, S. Outcome of tantalum rod insertion in the treatment of osteonecrosis of the femoral head with minimum follow-up of 1 year: a meta-analysis and systematic review. *J. Hip Preserv. Surg.* **2020**, *7*, 329−339.